CHEMICAL ENGINEERING TRANSACTIONS

VOL. 48, 2016

A publication of AIDIC
The Italian Association of Chemical Engineering
Online at www.aidic.it/cet

Guest Editors: Eddy de Rademaeker, Peter Schmelzer

**ISBN** 978-88-95608-39-6; **ISSN** 2283-9216

DOI: 10.3303/CET1648015

# Debris Throw Model for Accidental Explosions in a Complex Industrial Environment

Malte von Ramin*, Alexander Stolz

Fraunhofer Institute for High-Speed Dynamics, Ernst-Mach-Institut, EMI, Am Klingelberg 1, 79588 Efringen-Kirchen, Germany
Malte.von.Ramin@emi.fraunhofer.de

Alongside the accidental release of potentially hazardous substances, incidents evolving around the physical aspects of explosions are the second most reported type of hazard in the processing industry (ZEMA, 2002). The sudden failure of a component processing combustible gases exhibits a considerable risk to the operational safety of the affected process unit, if not the entire plant, and therefore to the health of affected personnel and public. In addition to the potential hazard associated with the blast wave propagation and the potential structural loss itself, the debris throw originating from the housing structure poses a significant threat to structures and personnel in the surrounding working environment in distances which may exceed the hazard-range of the blast wave itself. Further to the impending personal damage, other processing components or building structures can be affected, potentially causing cascading hazards. Insight into the break-up process during structural failure and the ensuing debris throw thus aids in defining safety distances important for a safe operation of the plant. This contribution describes a fast and efficient engineering methodology to determine the decisive safety ranges. For this purpose, dynamic threshold values for the break-up of building components are derived and the debris throw originating from masonry structures subjected to shock loads caused by the accidental gas explosion is described analytically. The methodology is demonstrated by picking up the example by Breitung and Yanez (2016) for an accidental release of hydrogen in a turbine hall. The debris throw from an affected masonry wall as part of an enclosure is exemplarily calculated.

## 1. Introduction

The debris throw resulting from an explosive event can be described using a simplified analytical methodology with the primary goal to define safety ranges. An equivalent loading density, defined by an equivalent high explosive charge mass and the room volume, represents an established approach to provide the loading in terms of pressure and impulse on the structural component, e.g. a masonry wall. The initial launch conditions for wall fragments are derived from yield-line-theory describing the wall behaviour subjected to bending forces. After the definition of the initial debris launch conditions – summarized in a fragment matrix pairing initial launch angle, maximum launch velocity and mass discretization – aerodynamic calculation yields the ranges of debris throw. Additional to the debris impact inhibiting a defined harmful energy content, the overall threat potential is derived by coupling with the threat from the blast wave. This leads to the definition of safe stand-off distances. The origin of this approach is well established in military applications concerned with the launch of ammunition fragments and transferred here to describe the initial launch conditions of masonry enclosures subjected to shock loads. The methodology can be adapted to other building materials such as concrete or glass as well. To describe the debris throw originating from a masonry structure on a simple structural system, the wall sketched out in Figure 1, left, is examined. The wall is laterally supported at top and bottom, defining a single-span flexural system. For simplicity, no vertical load on the wall is considered. To account for the influence of vertical compression on the bending capacity of a masonry wall, refer to Mayrhofer (1986) for details. It is acknowledged that the single-span system is the most simple system, however the most vulnerable to horizontal loads. In a wall represented by a two-span system the methodology is similar, only that the deformation at ultimate state is more complex, formed by a cruciform pattern established from yield-line theory.

Please cite this article as: von Ramin M., Stolz A., 2016, Debris throw model for accidental explosions in a complex industrial environment, Chemical Engineering Transactions, 48, 85-90 DOI:10.3303/CET1648015

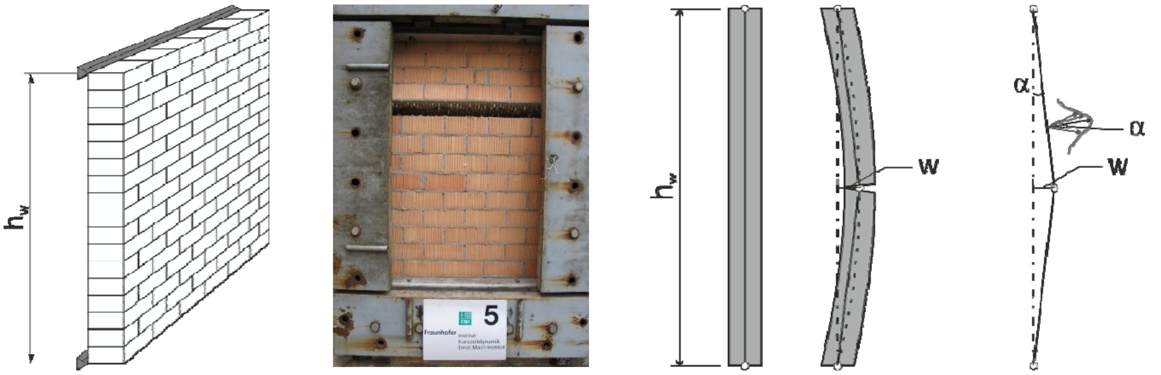


*Figure 1: Left, single-span wall system. Center, single-span wall system at the onset of the break-up process. Right, two-dimensional mechanical model at ultimate and fragment launch angle distribution.*

## 2. Loading conditions

For the scope of this contribution, it is assumed that the first parameter set, i.e. the initial loading conditions on the wall, are known. The loading conditions are best deduced from a Computational Fluid Dynamics (CFD) model, which can provide the transient non-uniform pressure distributions as they occur in internal explosions. Hence, wave reflections and focusing effects are included, thus yielding a realistic initial loading on the structural component. However, analytical methods, for example those described by Smith and Hetherington (1994) have the advantage that they might be less time consuming than numerical modelling. Precondition for debris throw originating from a masonry wall is that the loading – expressed by overpressure and corresponding impulse – exceeds the structural capacity of the wall. The analysis of the wall prior to the break-up point is easily done using iso-damage curves, indicating all pressure-impulse-combinations leading to the same deflection; in this case the deflection at ultimate state. Loading on the wall exceeding its structural capacity will start the break-up process with a deflection at ultimate limit state (ULS). From the ULS deflection, the initial launch angle for debris throw is directly deduced (Figure 1, right).

## 3. Initial launch conditions

The initial launch conditions for fragment trajectories are described by the initial launch angle of the debris throw and the fragment mass distribution. Both are summarized in a fragment matrix, tabulating the initial conditions for the subsequent trajectory calculations. In addition to the distribution of launch angle and mass classes, the debris launch velocity is the third initial condition for debris throw.

### 3.1 Launch angle

As visible in Figure 1, centre, a single-span masonry wall starts breaking up along the joints between brick and mortar. This is due to tension failure at the interface as the composite system wall = brick + mortar has very limited tensile capacity in the horizontal joints. It follows that the deformation at the onset of the break-up process can be assumed to provide the initial launch angle for the debris throw. As the curvature of a masonry wall subjected to bending at ULS is very shallow, a triangular deflection of a pin-jointed arch as depicted in Figure 1, right, represents the wall deflection with sufficient accuracy. Because masonry has almost no capabilities for deformations in the plastic domain, the ultimate displacement $w_u$ of a single-span masonry system subjected to explosion loads is expressed by a factored elastic deformation $w_{el}$, calculated from the curvature at the ultimate bending moment $M_0$, given by Eq(1), with the corresponding uniform load $p_0$, Eq(2).

$$M_0 = f_t \cdot d^2 / 6 \qquad (1)$$

$$p_0 = 1.3 \cdot f_t / \delta^2 \qquad (2)$$

With $f_t$ = tensile strength of masonry, $d$ = depth, $l$ = length, and $\delta$ = $l/d$ = slenderness of the section. The current Eurocode for masonry structures, EN 1996-1-1 (DIN, 2013) indicates a tensile strength of $f_t$ = $f_{xk1}$ = 0.2 kPa for solid brick masonry structures loaded parallel to the joints. The corresponding maximum deflection is provided by the elastic deformation $w_{el}$ of a single-span beam, Eq(3):

$$w_{el} = \frac{5 p_0 \cdot l^4}{384 EI} \qquad (3)$$

with $E = K_E f_k$ denoting the elastic modulus for masonry, which depends on its characteristic compression strength $f_k$ and a nominal value $K_E$ for the respective type of masonry (DIN, 2013), and $I = bd^3/12$ denoting the moment of inertia, where *b* is the width of the section.

According to Mayrhofer (1986), the ultimate deflection of a masonry wall panel subjected to high-speed dynamic loads is expressed by a multitude of the maximum elastic deflection, Eq(4):

$$w_u = 5\, w_{el} \tag{4}$$

The initial launch angle for debris origination from the brick wall is calculated from the rotational angle of the pin-jointed system shown in Figure 1, right, Eq(5):

$$\alpha = \tan^{-1}\left(\frac{w_u}{l/2}\right) \tag{5}$$

Based on previous research on reinforced concrete walls (Dörr et al., 2002), the angular distribution of masonry debris in horizontal and vertical direction is assumed to follow a Gauss normal distribution. According to the failure model depicted in Figure 1, right, the wall debris is divided into halves, such that the vertical angular distribution of debris throw is centered around the launch angle 90 ° ± $\alpha$ with a standard deviation $\sigma$ = 10 degrees. The launch angle distribution is the first variable parameter describing the initial launch conditions. The distribution of mass classes over the launch angle distribution forms the fragment matrix.

### 3.2 Debris mass distribution

For the purpose of the further analysis, the debris mass is clustered in distinct mass classes, or mass bins, containing the respective shares of wall debris within the bin intervals. The summation of all shares in all mass bins equals the total mass of the wall. Because of the small tensile strength in the joints of a masonry section, a wall subjected to a blast load past its horizontal bearing capacity ruptures mainly along the joints. It follows that the wall debris can be described by discrete numbers of bricks complemented by debris originating from the mortar in the joints. The mass classes are therefore established by bins containing the mass distribution shares of ¼ bricks, ½ bricks, single bricks, 2 bricks, and 3 bricks, respectively. Additional to the actual distribution of bricks inside the wall section considered, these mass classes represent the possibility of brick fracture or joined fragments. For solid bricks of density $\rho$ = 2.0 kg/dm³ measuring 240 mm x 115 mm x 113 mm, this results in bins containing masses of 1.56 kg, 3.12 kg, 6.24 kg, 12.48 kg, and 18.72 kg, respectively. In addition, the mortar fragments are accumulated in a single bin with a maximum mass of 50 g. For a solid brick wall section of 2.50 m height, 1.00 m width and 0.115 m thickness with a specific weight of 20 kN/m³, the accumulated masses are 75.8 kg of mortar and 499.2 kg of solid bricks. To establish the fragment matrix, the representative number of fragments is calculated. For example, for the mortar, accumulated in a single mass bin, this results in 75.8 kg / 0.05 kg/fragment = 1516 fragments (sum of all fragments in Table 1, column 2), which are distributed over the previously described launch angle distribution. The distribution of debris originating from bricks, associated to the previously defined mass bins, is assumed to follow again a Gauss normal distribution with the maximum at one brick and standard deviation in the neighbouring mass bins. Consequently, 95.5 percent of the mass falls into the width of 2 $\sigma$, encompassing the defined bins. With the previously outlined wall properties and the launch angles and mass classes, the fragment matrix displayed in Table 1 is established, assuming a rotational angle of $\alpha$ = ± 5 degrees at ultimate state.

*Table 1: Fragment matrix for a 2.5 m x 1.0 m x 0.115 m wall segment. Mass bins contain the number of fragments for each mass class.*

| Launch angle | Mass bin [kg] | | | | | |
|---|---|---|---|---|---|---|
| | 0.05 (mortar) | 1.56 (1/4 brick) | 3.12 (1/2 brick) | 6.24 (1 brick) | 12.48 (2 bricks) | 18.72 (3 bricks) |
| 65 | 36.60 | 0.71 | 0.94 | 0.64 | 0.23 | 0.06 |
| 70 | 110.70 | 2.14 | 2.83 | 1.94 | 0.71 | 0.18 |
| 75 | 192.59 | 3.73 | 4.93 | 3.37 | 1.23 | 0.31 |
| 80 | 268.30 | 5.19 | 6.86 | 4.70 | 1.72 | 0.43 |
| 85 | 74.90 | 1.45 | 1.92 | 1.31 | 0.48 | 0.12 |
| 90 | 149.80 | 2.90 | 3.83 | 2.62 | 0.96 | 0.24 |
| 95 | 74.90 | 1.45 | 1.92 | 1.31 | 0.48 | 0.12 |
| 100 | 268.30 | 5.19 | 6.86 | 4.70 | 1.72 | 0.43 |
| 105 | 192.59 | 3.73 | 4.93 | 3.37 | 1.23 | 0.31 |
| 110 | 110.70 | 2.14 | 2.83 | 1.94 | 0.71 | 0.18 |
| 115 | 36.60 | 0.71 | 0.94 | 0.64 | 0.23 | 0.06 |

### 3.3 Initial debris launch velocity

The initial debris launch velocity depends on the wall thickness *t*, the masonry density $\rho$, and the loading density, expressed by room volume *V* and equivalent TNT charge *NEQ* (net explosive quantity). Based on experimental research reported by Dörr et al. (2002), the initial debris launch velocity (DLV) is calculated by Eq(6) (van der Voort & Weerheijm, 2013), with the constant *C* = 525 m/s:

$$DLV = C\sqrt{\frac{NEQ}{V^{2/3}\cdot\rho\cdot t}} \quad (6)$$

To demonstrate the methodology, the contribution by Breitung and Yanez, "Analysis methodology for hydrogen accident scenarios in complex industrial environments" (2016) is used. It can be shown that a mass of 30 kg hydrogen equals approximately an equivalent TNT mass of 76 kg (Assael and and Kakosimos, 2010). Assuming an enclosure of the hydrogen tank inside the exemplary turbine hall with dimensions 7.5 m x 5.0 m x 2.5 m, wall thickness *t* = 0.115 m, and brick density $\rho$ = 2,000 kg/m³ results in a debris launch velocity of DLV = 66.4 m/s. Originating with the DLV, the debris enters the flight phase, described by the respective trajectories.

## 4. Debris propagation

In relation to the wide-spread debris distribution, it is assumed that the masonry wall propagates from the centre of a point source. The flight trajectories for the debris throw and the resulting debris mass distribution are calculated originating from that point source.

### 4.1 Flight trajectories

The trajectories describing the debris flight in air are calculated for the number of fragments contained in each mass bin, originating with the respective launch angle and DLV from the point source. The trajectories are primarily governed by gravity and air drag, where the air drag is directed against the flight direction, Figure 2, left. The air drag force $F_w$ depends on the air drag coefficient $c_w$, the exposed cross section *A*, and the density of air, $\rho$. Force equals the time derivative of the impulse. The drag force is proportional to the product of displaced air mass per time and velocity. Using the air drag coefficient $c_w$, the drag force $F_w$ is given by Eq(7):

$$F_w = 0.5\cdot c_w\cdot\rho\cdot v^2\cdot A \quad (7)$$

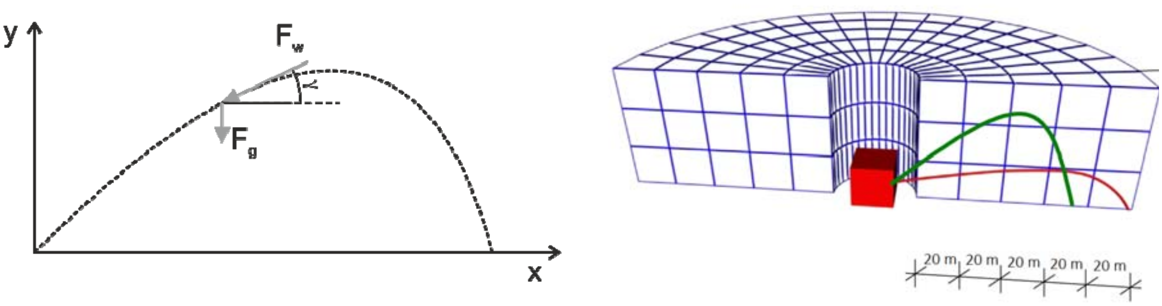


*Figure 2: Left, Trajectory of a single fragment indicating gravity and air drag. Right, Exemplary discretization of the spatial surroundings to monitor flight trajectories (Dörr et al., 2002).*

The angle $\gamma$ (Figure 2, left) describes the inclination of the direction of motion. The horizontal and vertical components of the acceleration are defined by Eq(8) and Eq(9), which can be transformed into the coupled set of differential equations Eq(10) and Eq(11) by implementing Eq(7) and defining the specific mass $q = m/A$ (Dörr et al., 2002).

$$a_x = v'_x = -F_w/m\cdot\cos\gamma \quad (8)$$

$$a_y = v'_y = -F_w/m\cdot\sin\gamma - F_g/m \quad (9)$$

$$v'_x = \frac{dv_x}{dt} = -0.5\cdot c_w\cdot\rho\cdot v\cdot v_x\cdot\frac{1}{q} \quad (10)$$

$$v'_y = \frac{dv_y}{dt} = -0.5 \cdot c_w \cdot \rho \cdot v \cdot v_y \cdot \frac{1}{q} - g \qquad (11)$$

The drag coefficient $c_w$ depends on the debris shape, the flight pattern (relative orientation in air) and its velocity in air (Janzon, 1971). As the vast majority of debris originating from the masonry wall is of approximately cubic shape, it is safe to assume this the governing shape. The differential equations Eq(10) and Eq(11) are solved numerically in a computer routine, querying the drag coefficient depending on the respective velocity range using a lookup table.

### 4.2 Projection on exposed site

The flight trajectories are continuously monitored on a three dimensional grid, depicted in Figure 2, right. The grid is discretized in variable angular segments with variable length and height. At each point in time during the debris flight, the mass and current velocity – and therefore the energy of the singular fragments – are known.

## 5. Damage potential

Following through with the previous example, a scenario is evaluated where the hydrogen explosion is taking place inside an enclosure within the turbine hall. The enclosure is built from reinforced concrete walls and a failing masonry wall segment to be evaluated. This hazard scenario poses a threat to surrounding processing components such as pipes, valves, and tanks in addition to exposed building construction and personnel. The scenario is modelled in a specialized newly developed software tool that bases on the previously described methodology transferred to the application of process industry safety. The methodology itself has successfully been applied in the field of explosion safety (Brombacher, Radtke & Steyerer, 2013). To demonstrate the potential threat in the vicinity of the explosion, some exemplary components are included in the model, representing other building or processing components and personnel within the turbine hall, i.e. within a space confined by 45 m x 84 m (Figure 3).

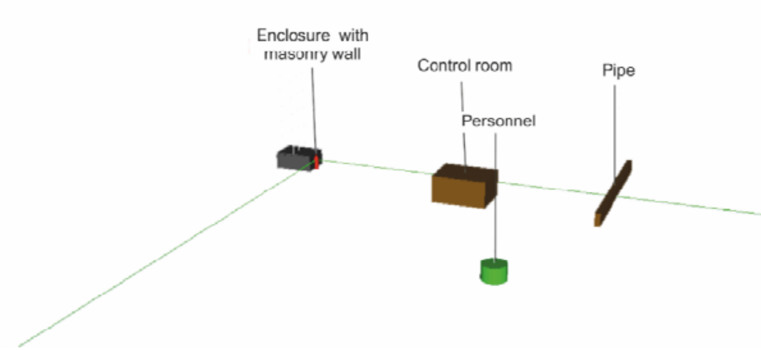


*Figure 3: Exemplary scenario showing the masonry wall (debris source) and surrounding components.*

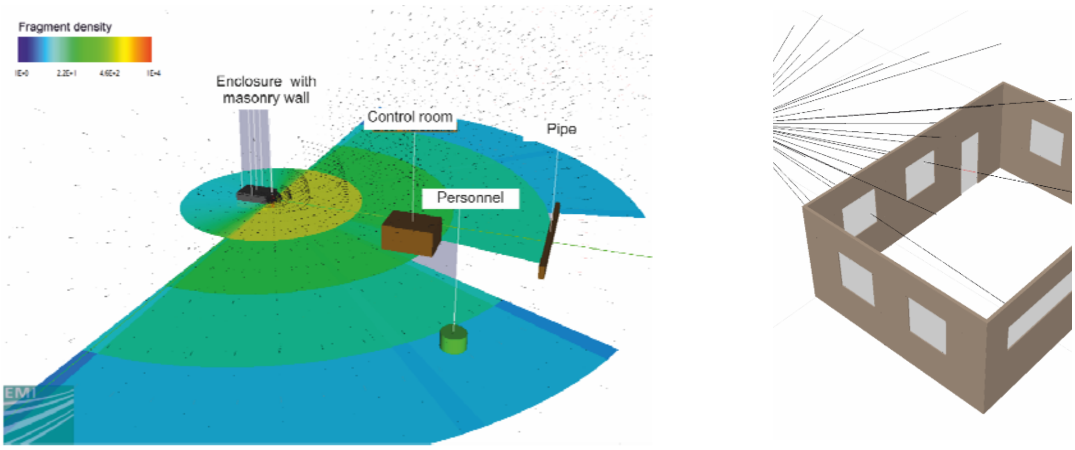


*Figure 4: Left, fragment density with E ≥ 79 J on ground after exemplary wall break-up. Right, penetration of structural components of the "control room" by critical fragments originating from the masonry wall.*

The threat of personal injury caused by debris throw is calculated based on a criterion that defines an area as critical if the density of fragments exceeds an energy content of E ≥ 79 kJ per 56 m² (NATO Standardization Agency, 2006). Figure 4, left, shows the fragment density matching this criteria along with the fragment trajectories (black dotted lines). The colour mapping in Figure 4 indicates different fragment densities on the ground, from which safety distances are derived. The safety distances are calculated based on the fragment density, because the density defines – complemented by the threat exposure – the damage probability. Equivalent to the assessment of personal injury, the impact energy of the fragments is used to derive the level of damage to structural components. For example, the possible penetration of building components and materials– and therefore the potential for cascading effects originating from fragment impact can be calculated as shown in Figure 4, right

## 6. Conclusions

For the assessment of explosion effects in a process industry environment, it is vital to describe the physical effects that pose the hazardous threat, chiefly the blast wave propagation and debris throw. The methodology outlined in this contribution describes the debris throw hazard originating from the break-up of a masonry wall subjected to blast loads. Beginning with the ultimate limit state condition of the wall, the initial debris launch conditions are defined by the initial launch angle, launch velocity, and fragment mass distribution. The subsequent trajectory calculations yield the final fragment distribution in debris flight direction along with the associated energy content, which forms the principal parameter for possible damage caused by fragment impact on process units, building structures, or personnel in the vicinity of the explosion. Presented here for a masonry structure, the methodology can be adapted to further construction materials.

### References


Assael M.J., Kakosimos K.E., 2010, Fires, Explosions, and Toxic Gas Dispersions, CRC Press, Boca Raton, FL, USA

Breitung W., Yanez J., 2016, Analysis Methodology for Hydrogen Accident Scenarios in Complex Industrial Environments, contribution to Loss Prevention 2016, Freiburg, Germany

Brombacher B., Radtke F.K.F. & Steyerer M., 2013, ISIEMS 2013: Hazard and damage analysis of a VBIED attack on a hotel using ESQRA-GE 3.0.

DIN Deutsches Institut für Normung e.V., 2013, Eurocode 6: Design of masonry structures – Part 1-1: General rules for reinforced and unreinforced masonry structures; German version EN 1996-1-1:2005+A1:2012, EN 1996-1-1:2005+A1:2012, Beuth Verlag, Berlin, Germany.

Dörr A., Michael K., Gürke G., 2002a, Experimental Investigation of the Debris Launch Velocity from Internally Overloaded Concrete Structures, Final Report DLV 4-2002 E 09/02, Fraunhofer-Institut für Kurzzeitdynamik, Ernst-Mach-Institut, Freiburg, Germany.

Dörr A., Michael K., Gürke G., Mayrhofer C., 2002b, Schadensmodell für Trümmerwurf bei Explosions-ereignissen, Trümmerwurfmodell E 06/03, Fraunhofer-Institut für Kurzzeitdynamik, Ernst-Mach-Institut, Freiburg, Germany.

Janzon B., 1971, Retardation of fragments in air FOA Rapport A 2539-44, FOA, Stockholm, Sweden.

Mayrhofer C., 1986, Dynamisches Tragverhalten von Mauerwerk bei horizontaler Belastung: Schlußbericht zum Auftrag "Bauliche Schutzmaßnahmen" der Schutzkommission beim Bundesminister des Innern 1977 - 1985 E 5/86, Fraunhofer Institut für Kurzzeitdynamik, Ernst-Mach-Institut, Freiburg, Germany.

NATO Standardization Agency, 2006, Manual of NATO safety principles for the storage of military ammunition and explosives (AASTP-1), Allied Ammunition Storage and Transport Publication, NATO Standardization Agency, Brussels, Belgium.

Smith P.D, Hetherington J.G., 1994, Blast and Ballistic Loading of Structures, Butterworth-Heinemann, Oxford.

van der Voort M., Weerheijm J., 2013, A statistical description of explosion produced debris dispersion, International Journal of Impact Engineering, vol. 59, pp. 29–37.

Zentrale Melde- und Auswertestelle für Störfälle in verfahrenstechnischen Anlagen, 2002, Zusammenfassende Auswertung der meldepflichtigen Ereignisse 1993-2002, Umweltbundesamt, viewed 21 August 2015, <http://www.umweltbundesamt.de/sites/default/files/medien/376/dokumente/zusammen-fassende_auswertung_der_meldepflichtigen_ereignisse_1993-2002.pdf>.